

# X rays from radiative electron capture into continuum states in relativistic heavy-ion collisions

H. Tawara,<sup>1</sup> T. Azuma,<sup>2</sup> T. Ito,<sup>2</sup> K. Komaki,<sup>2</sup> Y. Yamazaki,<sup>2</sup> T. Matsuo,<sup>3</sup> T. Tonuma,<sup>4</sup> K. Shima,<sup>5</sup> A. Kitagawa,<sup>6</sup>  
and E. Takada<sup>6</sup>

<sup>1</sup>National Institute for Fusion Science, Nagoya 464-01, Japan

<sup>2</sup>College of Arts and Sciences, University of Tokyo, Komaba, Tokyo 153, Japan

<sup>3</sup>Tokyo Medical and Dental University, Yushima, Tokyo 113, Japan

<sup>4</sup>Institute of Physical and Chemical Research, Wako-shi, Saitama 371-01, Japan

<sup>5</sup>Accelerator Center, University of Tsukuba, Tsukuba 305, Japan

<sup>6</sup>National Institute of Radiological Sciences, Anagawa, Chiba 263, Japan

(Received 12 August 1996)

Continuum x rays originated from radiative electron capture into continuum states (RECC) of relativistic  $\text{Ne}^{10+}$  ions have been observed. It has been found that the intensities of x rays decrease as their energy increases and the observed spectra show a clear edge which corresponds to the maximum energy transferred to free electrons under energetic projectile-ion collisions. The edge becomes dramatically sharp as the incident projectile energy decreases from 290 to 75 MeV/amu, indicating that the cross sections for RECC sharply increase at low projectile energies, which is in agreement with the theoretical expectation. [S1050-2947(97)07101-1]

PACS number(s): 34.70.+e

## I. INTRODUCTION

In energetic heavy-ion-neutral-atom collisions, various types of x rays have been observed so far. The first are the characteristic x rays which originate from the projectile ions or target atoms and are well defined in energy but almost independent of the collision energy, though their intensities do depend strongly on it. Various features of these characteristic x rays and their production mechanisms under heavy-ion impact have been investigated in detail and summarized [1].

The second are also characteristic, combined with both projectile and target, but they have the energy distributions much broader than the characteristic x rays which are caused through collisional dynamics. One is x rays due to the electron capture into the discrete states of projectile ions, called radiative electron capture (REC) [2–5], from the target atoms. Another example is the quasimolecular x rays [6] which are generated in quasimolecules formed during slow, heavy-ion-atom collisions and is dominant only at slow collisions.

The third are continuous x rays whose shapes depend on both the projectile ion and the target atom and have high-energy ends characteristic to the collision velocity. One is the secondary electron bremsstrahlung (SEB) [7,8] which is generated through scattering of secondary electrons produced in the primary projectile-ion-target-atom collisions and thus observed only in solid targets. The energy of the SEB spectrum extends up to the highest energy determined by the maximum momentum transfer to the target (quasi-free) electrons, given as  $T_s = 2mv_p^2$ , where  $m$  is the electron rest mass and  $v_p$  is the projectile velocity relative to the target electrons. The other is bremsstrahlung of electrons bound to the target which are scattered by the incident projectile Coulomb field and whose highest energy is equal to that corresponding to the projectile velocity,  $T_e = (\frac{1}{2})mv_p^2$ . This is in various ways called primary bremsstrahlung (PB)

[9,10], quasi-free-electron bremsstrahlung (QFEB) [11], or radiative ionization (RI), depending on the analogy of the production mechanisms. It can also be considered to be due to radiative electron capture into continuum (RECC) [12], analogous to REC into the discrete states mentioned above. It is clear that the SEB tails extend up to four times higher energies than those for RECC.

Up to now, very few investigations have been reported on continuum x rays from RECC, in particular at relativistic collision energy region involving heavy projectile ions [9,13].

In the present work we report on the observations and investigations of the characteristics of the continuum x rays originated from RECC which are generated in relativistic  $\text{Ne}^{10+}$  ion-low-Z- (solid Be, C) target collisions.

## II. EXPERIMENTAL PROCEDURES

The present experiment has been performed at the Heavy Ion Medical Accelerator at Chiba (HIMAC) facility at National Institute of Radiological Sciences which consists of two ion sources, a linear accelerator and two independent but similar synchrotrons capable of accelerating ions up to  $\text{Ar}^{18+}$  and is devoted principally to medical treatments and biological applications, a part of which is used for other scientific work.

Seventy-five-, 150-, and 290-MeV/amu  $\text{Ne}^{10+}$  projectile ions of  $10^5$ – $10^6$  particles per second with the repetition of 2 or 3.3 s provided from the HIMAC facility are focused down to roughly 5 mm in diameter on target foils which are 0.2-mm-thick beryllium or 0.10- and 0.20-mm-thick carbon. The absolute intensities of the incident projectile ions are monitored with an ionization chamber upstream from the target and also with a deep Faraday cup downstream and their charge is integrated, with an accuracy of about 30%, during measurements. The x rays generated have been observed at  $90^\circ$  with respect to the projectile ions with an ultrapure ger-

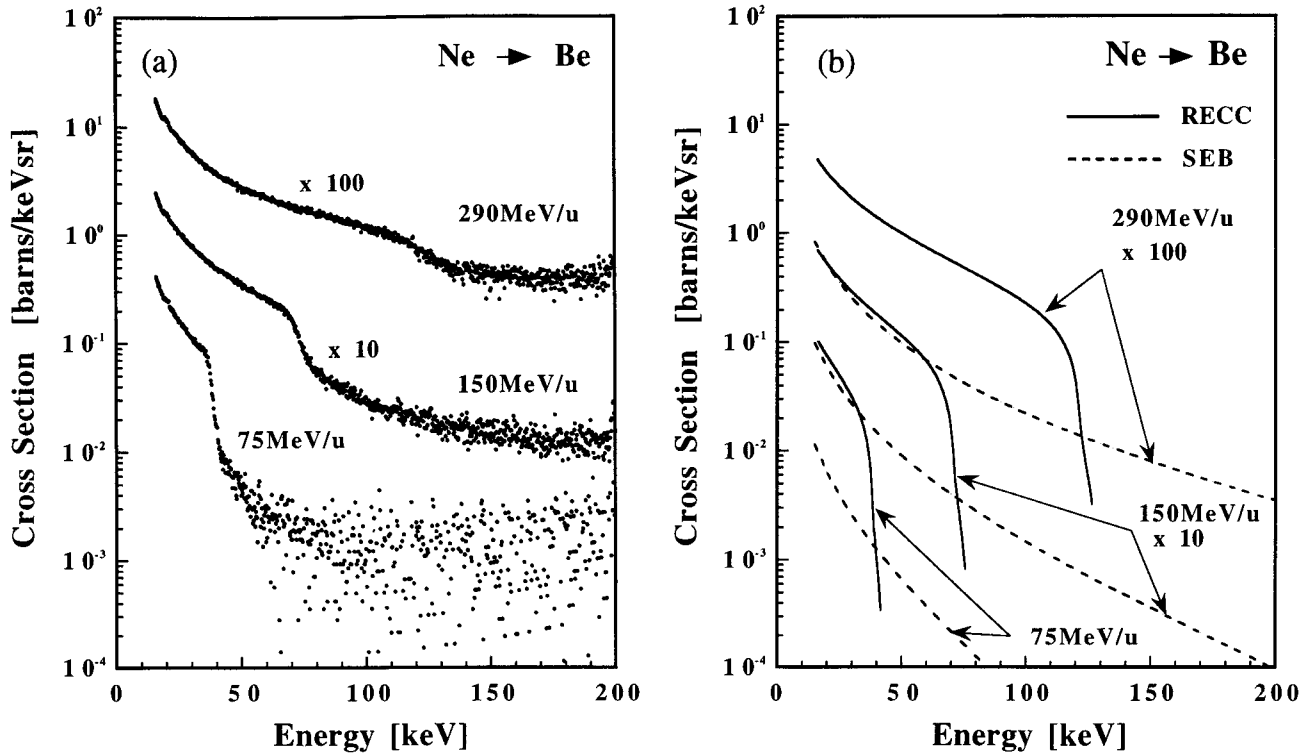


FIG. 1. The observed (a) and calculated (b) RECC x-ray spectra from 75-, 150-, and 290-MeV/amu  $\text{Ne}^{10+} + \text{Be}$  collisions as a function of the x-ray energy. In (b) are also shown the SEB spectra. Note that the intensities of the spectrum are shown by proper multiplication factors in order to avoid the overlapping.

manium detector with a resolution of about 650 eV for 122-keV x rays. The overall efficiencies of the detector are corrected for a 6- $\mu\text{m}$ -thick Mylar window and 8-cm-long air path. The detector solid angle subtended over the target is about 18 mrad. During the observation the pileup of x-ray pulses in the detector is limited to be less than 5%.

### III. RESULTS AND DISCUSSION

The photons emitted from REC and RECC have the same physical origin which is due to the electron capture into the projectile ions, followed by x-ray emission. The difference is the final state, either the discrete state (REC) or the continuum state (RECC), of an electron in the projectile ions. Consequently, the cross sections for REC and RECC differently depend on the projectile charge  $Z_p$  and projectile velocity  $v_p$ , as discussed by Shakeshaft and Spruch [14]. These have the following forms at asymptotically high-energy region:

$$\sigma(\text{REC}) \propto Z_p^5 Z_t / v_p^5,$$

$$\sigma(\text{RECC}) \propto Z_p^2 Z_t / v_p^2,$$

where  $Z_t$  represents the target charge (or the number of target electrons). The RECC in the present relativistic  $\text{Ne}^{10+} + \text{Be}$  collisions can be expected to be far dominant over REC. This

feature has been confirmed in the present work where practically no REC peaks can be seen in the observed x-ray spectrum. Note that both REC and RECC x-ray yields increase linearly with the target thickness, which has been confirmed in the present work.

RECC process results in the production of continuum photons (x rays) with the maximum energy which corresponds to the maximum energy transferred to a quasi-free-electron through collisions with projectile ions. As the electrons are bound in the neutral-atom targets, then the Compton profiles of their electrons influence the distributions and shapes of the RECC spectrum, in particular in the maximum energy region of x rays. The maximum energy of x rays emitted from REC and RECC depends on various parameters and can be given as follows:

$$E(h\omega)_{\text{cm}} = E_p - \gamma E_t + m_0 c^2 (\gamma - 1), \quad (1)$$

where  $E_p$  is the binding energy in projectile after capture,  $E_t$  the binding energy in target before capture,  $m_0 c^2$  the electron rest mass (=511 keV),  $\gamma^2 = 1/(1 - \beta^2)$ ,  $\beta = v_p/c$ , and  $c$  is

TABLE I. Calculated RECC edge energies in  $\text{Ne}^{10+}$  projectile collisions [see Fig. 1(a)].

Incident projectile energy (MeV/amu)	75	150	290
Edge energy (keV) (calculated)	38	71	121

the speed of light. In the present experiments,  $\gamma$  ranges from 1.08 to 1.32 over 75–290-MeV/amu collision energies. The first and second terms represent the final and initial binding energies and the third the kinetic energy of an electron with the velocity equivalent to the projectile ions. Naturally the first term vanishes for RECC.

In the present (relativistic) energy range, the photon energy observed at the laboratory angle  $\theta_{\text{lab}}$  is given as follows:

$$E(h\omega)_{\text{lab}} = E(h\omega)_{\text{cm}} / [\gamma(1 - \beta \cos \theta_{\text{lab}})]. \quad (2)$$

In comparing the experimentally observed x-ray spectra with theories in heavy-ion collisions, we have to check and to know the contributions of SEB and background Compton-scattered nuclear  $\gamma$  rays. SEB is understood reasonably well and its spectrum can be evaluated. The SEB intensity is roughly given as follows [8,9]:

$$\sigma(\text{SEB}) \propto Z_p^2 Z_t^2 / v_p^2.$$

We should note that SEB is proportional to the square of the target thickness ( $Z_t^2$ ), in contrast with the REC and RECC. In the present experiments, namely, in high collision energy and relatively thin solid target situations, the intensities of the observed x rays below the RECC edges have been confirmed to increase almost linearly with the target thickness, indicating that the SEB contribution is relatively small. Indeed the calculation shows that the SEB is roughly more than one order of magnitude smaller than the RECC intensities observed in the present work (see Fig. 1). Furthermore, the SEB contribution to the observed RECC spectrum can be expected to become much smaller if taking into account the fact that high-energy (100–200 keV), secondary electrons produced in such relativistic collisions can pass, without much scattering, through the target foil chosen in the present work [15].

Measurements with an empty target holder indicate that the Compton-scattered  $\gamma$  rays at the energy above the RECC edge have been found to come mostly from the surroundings. In fact, the measured x-ray intensities above the RECC edge in the original spectra (before subtracting the background x rays) are found to be independent of the target thickness, suggesting that indeed these x rays have the origin of nuclear backgrounds from the surroundings.

Typical RECC x-ray spectra observed in the present work at 75-, 150-, and 290-MeV/amu  $\text{Ne}^{10+}$  projectile ions incident on a thin Be foil are shown in Fig. 1(a). These spectra, with backgrounds mostly of nuclear origin subtracted, show some common features: continuous distribution up to the maximum energy which depends on the projectile-ion energy [see Eq. (1)] and, then, sudden decrease above it, forming a sharp edge. The contribution above this maximum edge is mostly due to the nuclear backgrounds. These observed energy edges dependent on the collision velocity seem to be in good agreement with the edges calculated from Eqs. (1) and (2) (see Table I and Fig. 1).

The observed RECC spectrum shapes are found to be practically the same for both Be and C targets. A comparison of the observed RECC x-ray yields from Be and C targets suggests that RECC yields are indeed proportional to the number of the electrons in the targets.

The spectrum shapes of RECC can be calculated in a way similar to that given by Anholt and Gould [9] which is based upon the Bethe-Heitler bremsstrahlung formula (2BN) given by Koch and Motz [16], combined with the momentum distributions (Compton profile) of the electrons in a free target atom [17].

It should be noted that the detailed shapes of the spectrum edge regions depend upon the Compton profile of the capturing electrons in the target as well as some experimental conditions such as the detector angles subtended and the corresponding Doppler shift. All of them tend to stretch the spectrum and decrease the photon intensities near the continuum edges more slowly.

The general shapes of the calculated spectra are shown in Fig. 1(b), together with the SEB spectra calculated using bremsstrahlung formula (3BN) of Koch and Motz [16], as described by Anholt and Gould [9]. In particular, the relative intensity distributions of RECC at 150- and 75-MeV/amu collisions are quite nicely fitted with the calculated spectra. Yet the absolute intensities of the calculated RECC spectra are a factor of 2–3 smaller than those observed, as already pointed out by Anholt and Gould [9]. On the other hand, that at 290 MeV/amu seems to be in disagreement, particularly at the highest-energy region near the continuum ends. This may be due to the fact that the contribution of the nuclear-scattered  $\gamma$ -ray background is sufficient at the highest-energy region, in particular near the RECC edges.

Further detailed investigations including different projectile ions up to  $\text{Si}^{14+}$  and  $\text{Ar}^{18+}$  ions at various collision energies are under way.

In conclusion, we have observed the continuum x rays from RECC of heavy-ion collisions at relativistic energies which show very sharp edges at the high-energy end region corresponding to the maximum energy transferred to free electrons from the projectile ions and compared their features as well as spectra with the calculated spectra based on the bremsstrahlung due to the target electrons scattered by the incident projectile ions which is in reasonable agreement with the observation.

## ACKNOWLEDGMENTS

The present work was supported by one of the Collaboration Programs at HIMAC (P-014). Finally, the present authors would like to express appreciation for the contribution from many colleagues, in particular Dr. T. Murakami and the staffs of the HIMAC facility, who provided the projectile ion beam for the present work, Dr. A. Warczak of Jagiellonian University, who joined a part of the present work, Dr. K. Ishii of Tohoku University, who gave some accounts of his RECC calculations, and Dr. T. Shirai of the Japan Atomic Energy Institute for his calculation of REC cross sections. Discussion with Dr. J. Burgdörfer of the University of Tennessee is also highly appreciated.

- [1] J. D. Garcia, R. J. Fortner, and T. M. Kavanagh, *Rev. Mod. Phys.* **45**, 111 (1973).
- [2] H. W. Schnopper, H. D. Betz, J. P. Delvaille, K. Kalata, A. R. Sohval, K. W. Jones, and H. E. Wagner, *Phys. Rev. Lett.* **29**, 898 (1972).
- [3] D. H. Jakubassa and M. Kleber, *Z. Phys. A* **273**, 29 (1975).
- [4] H. Tawara, K. Kawatsura, and P. Richard, *Phys. Rev. A* **26**, 154 (1982).
- [5] Th. Stöhlker, C. Kozhuharov, P. H. Mokler, A. Warczak, F. Bosch, H. Geissel, R. Moshhammer, C. Scheidenberger, J. Eichler, A. Ichihara, T. Shirai, Z. Stachura, and P. Rymuza, *Phys. Rev. A* **51**, 2098 (1995).
- [6] F. W. Saris, W. van der Weg, R. Laubert, and H. Tawara, *Phys. Rev. Lett.* **28**, 717 (1972).
- [7] F. Folkmann, J. Birggreen, and A. Kjeldgaard, *Nucl. Instrum. Methods* **119**, 117 (1974).
- [8] K. Ishii, M. Kamiya, K. Sera, S. Morita, and H. Tawara, *Phys. Rev. A* **15**, 2126 (1976).
- [9] R. Anholt and H. Gould, *Adv. At. Mol. Phys.* **22**, 315 (1986).
- [10] C. R. Vane, S. Datz, P. F. Dittner, J. Giese, N. L. Jones, H. F. Krause, T. M. Rosseel, and R. S. Peterson, *Phys. Rev. A* **49**, 147 (1994).
- [11] A. Yamadera, K. Ishii, K. Sera, M. Sebata, and S. Morita, *Phys. Rev. A* **23**, 24 (1981).
- [12] L. A. Andersson and J. Burgdörfer, in *The Physics of Electronic and Atomic Collisions*, edited by T. Andersen, B. Fasttrup, F. Folkmann, H. Knudsen, and N. Andersen, AIP Conf. Proc. No. 295 (AIP, New York, 1993), p. 595.
- [13] J. Eichler and W. E. Meyerhof, *Relativistic Heavy Ion Collisions* (Academic, New York, 1995).
- [14] R. Shakeshaft and L. Spruch, *Rev. Mod. Phys.* **51**, 369 (1979).
- [15] L. Pages, E. Bertel, H. Joffre, and L. Sklaveinties, *At. Data* **4**, 1 (1972).
- [16] H. W. Koch and J. W. Motz, *Rev. Mod. Phys.* **31**, 920 (1959).
- [17] F. Biggs, L. B. Mendelsohn, and J. B. Mann, *At. Data Nucl. Data Tables* **16**, 201 (1974).